Functional Materials 14, No.4 (2007)

Thermal lag of the growth furnace heating assembly at CsI(Na) crystal growing from constant melt volume on a seed

V.I.Goriletsky, V.V.Vasilyev, O.Ts.Sidletskiy, M.M.Tymoshenko, V.I.Sumin

Institute for Scintillation Materials, STC "Institute for Single Crystals", National Academy of Sciences of Ukraine, 60 Lenin Ave., 61001 Kharkiv, Ukraine

Received October 22, 2007

Thermal lag of the heater — crucible — crystal system has been determined at a large size CsI(Na) single crystal growing from constant melt volume on a seed. It has been established that during radial growth the temperature stabilization time at the bottom heater power variation is 1.3 times shorter than that at the side heater power variation. During axial growth, the time difference decreases, drops to 0 at cylinder height about 50 mm, and, then, reverses its sign.

Определено время температурной инерции системы "нагреватель – тигель – кристалл" (элементов теплового узла печи) при выращивании крупногабаритных монокристаллов CsI(Na) на затравке из расплава постоянного объема. Установлено, что на стадии радиального роста слитка время стабилизации температуры при ее изменении на донном нагревателе в 1.3 раза короче, чем от бокового нагревателя. При аксиальном росте кристалла разница во временах сокращается, затем становится равной нулю при высоте цилиндрической части ≈50 мм. При дальнейшем увеличении высоты кристалла ситуация изменяется на противоположную.

Automated continuous method of alkali halide crystals (AHC) growing realized in the industrial "ROST" type equipment [1–3] is being applied for several last decades for needs of modern materials science [4, 5]. The crucible and crystal rotation provides thermal field symmetry within the crystal and the melt and promotes the natural convection of the melt and the dopant. The constant melt level in the crucible provided by the raw material feeding sustains the stability of thermal conditions at the phase boundaries. The method provides stationary conditions near the crystallization front in order to obtain ingots with high structure perfection and homogeneous activator distribution throughout the volume. Automated control system ensures growing of large crystals with reproducible dimensions and diameter maintenance precision within at least 1.5 %.

The growth furnace in a "ROST" type apparatus (Fig. 1) comprises the two basic water cooled parts. The thermal camera with crucible (1), periphery circular vessel (PCV) (2), side heater (3), and bottom one (4), melt (5) and heater thermal insulation (6) are situated in the lower part. The large size crystal (7) is situated in the upper part. Thus, the furnace construction predefines the thermal flux direction from heaters through the crucible, melt, and crystal to the upper case.

The crystal diameter automated control at discrete pulling of the crystal and discrete melt feeding is maintained indirectly — by bottom heater (t_{bot}) temperature correction based on comparison of melt level lowering value with a predetermined one in every

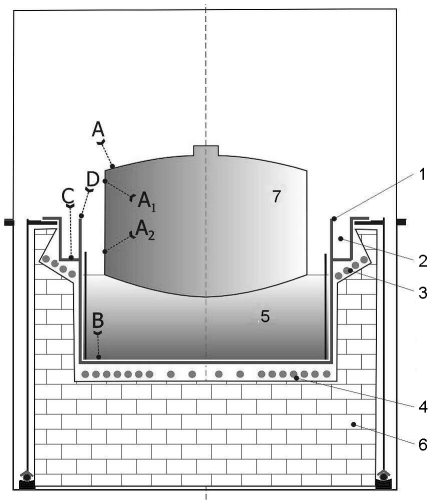

Fig. 1. Scheme of a ROST type apparatus and measurement points at growing crystal (A, A_1 and A_2) and crucible elements (B, C, D). 1 – Crucible; 2 – PCV; 3 – side heater; 4 – bottom heater; 5 – melt; 6 – thermal insulation of heaters; 7 – crystal.

cycle [9]. The basic task of the side heater (t_{side}) is local heating of PCV bottom (Fig. 1, pos. 2) and raw material melting to compensate the melt level lowering after crystal discrete pulling and, thus, to maintain the constant melt level during the whole growth process.

At such construction, the t_{bot} automated correction curve at large crystal growth [10] evidences substantial changes of heat removal intensity from the ingot at the cylinder growth. That is why it is necessary to obtain information on thermal lag of both heaters in dependence on crystal dimensions. That information makes it possible to study the heat transfer dynamics and to optimize the algorithm of the automated diameter control system (ACS). These studies became possible due to adaptation of IR pyrometry to the conditions of AHC growing [6–8].

The experiments on forced change of heater temperatures by 2°C and registration of response in different parts of the crystal and crucible (Fig. 1) were carried out using a Raytek Marathon MA2SC pyrometer out during the crystal growing process. The experimental data being transferred to PC and processed using a "Raytek Multidrop" software. The temperature before the correction was taken as zero.

It is known from the prior experiments [6] that IR pyrometry of upper and side crystal surfaces is possible only if the condensate thickness is at least 200 μm. The visible boundary of the crystal surface region satisfying this condition is shown by the arrows (Fig. 2). The crystal surface is semitransparent between the boundary and crystal edge, and measurements in this region contains a large experimental error. The basic measurements at the crystal di-

$Ø_{cryst}/H_{cyl}$, mm	Bottom heater		Side heater	
	τ, min	Registration, $\Delta t_{pyrometer}$, °C	τ, min	Registration, $\Delta t_{pyrometer}$, °C
$Ø_{cryst}$ =150	4,25	1,6	6	0,5
$Ø_{cryst}$ =280	4,35	1,4	6	0,7
H_{cyl} =10	4.6	1,1	6,6	1,1
H_{cyl} =20	5,65	1,1	6,8	0,95
H_{cyl} =120	14	0,9	10,5	0,5

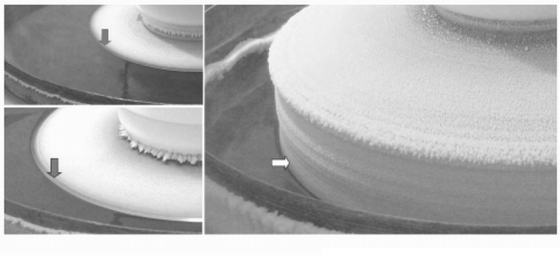

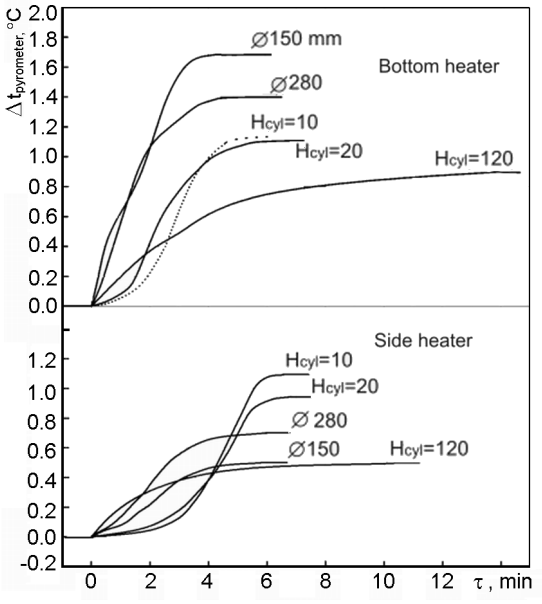

Fig. 2. Thermal lag and temperature change value in the point A at different growth stages (crystal diameter = 150, 280 mm, H_{cyl} = 10, 20, and 120 mm) at temperature change of bottom and side heaters by 2°C. Photo: growing crystal view at different growth stages. The results of measurements are shown in the Table.

H_{cyl}, mm	Measurement point	Bottom heater		Side heater	
		τ, min	Registration, $\Delta t_{pyrometer}$, °C	τ, min	Registration, $\Delta t_{pyrometer}$, °C
H_{cyl} =120	A	14	0,9	10,5	0,5
	A_1	16,5	0,9	9	0,65
	A_2	13,5	1,1	8,8	0,6

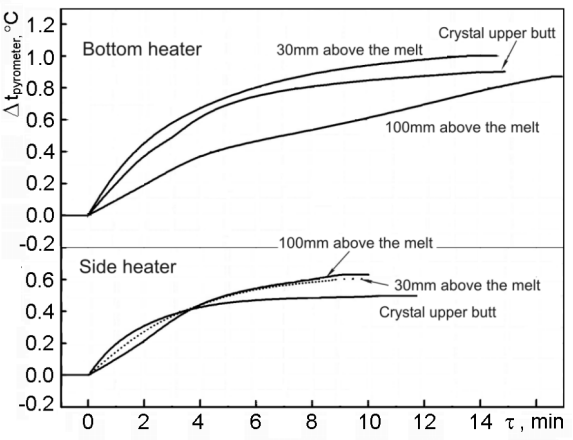

Fig. 3. Temperature stabilization time and temperature change values in the points A, A_1 and A_2 at H_{cyl} = 120 mm at bottom and side heater temperature variation by 2°C. The measurement data are presented in the Table.

ameter of 150 and 280 mm and cylinder height (H_{cyl}) 10, 20, and 120 mm (Fig. 1, point A) were conducted at upper crystal surface at the distance 15–20 mm from the crystal edge at different growth stages. The side crystal surface at H_{cyl} = 120 mm was studied also in the points A_1 and A_2 at 30 and 100 mm distances from the melt surface, respectively. Moreover, measurements were carried out in points at crucible bottom, PCV bottom, PCV wall (Fig. 1, points B, C, and D, respectively). Results of these measurements will be presented below.

Let us subdivide the obtained data concerning thermal lag time and temperature difference value into several parts.

The first one is presented in Fig. 2 for measurements in point A (at crystal upper surface) at crystal diameter 150, 280 mm and H_{cyl} = 10, 20 and 120 mm. It can be seen that thermal lag of both heaters (τ) increases proportionally to crystal dimensions, in contrast to temperature change value (Δt_{pyr}) measured by pyrometer. It should be noted that shorter τ values are obtained for the basic (bottom) heater at all the stages except for the last one (H_{cyl} = 120 mm) where the side heater acts faster. Also, τ(Δt_{pyr}) curves for the bottom heater at H_{cyl} = 10 and 20 mm differ in character

H_{cyl}, mm	Measurement point	Bottom heater		Side heater	
		τ, min	Registration, $\Delta t_{pyrometer}$, °C	τ, min	Registration, $\Delta t_{pyrometer}$, °C
H_{cyl} =120	B	4	1,9	7,5	0,8
	C	8	0,6	2,5	1,6
	D	10	0,9	4	1,2

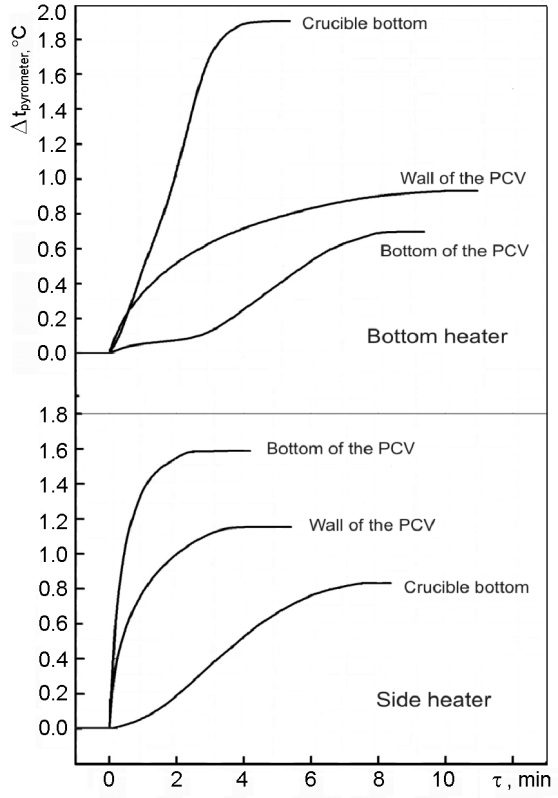

Fig. 4. Stabilization time and temperature change values measured in points C, B, and D at crucible surface at variation of heater temperatures by 2°C. The measured data are presented in the Table.

from those for crystal diameter 150 and 280 mm and H_{cyl} = 120 mm for the side heater. This evidences heat transfer intensification in the furnace at appearance of the side crystal surface not covered with condensate above the melt.

Considering the trend of τ(Δt_{pyr}) curves for bottom and side heaters in the next group of data (Fig. 3) in the points A, A_1 and A_2 at various crystal surfaces (at H_{cyl} = 120 mm), we can make the conclusion that the heat transfer mechanism from different heaters to these points is different. Herein, the bottom heater heats mainly the melt, thereby compensating the heat removal from the crystal. The melt / crystal phase interface is transparent for radiant heat flux and Δt_{pyr} value is 1.1°C, however, τ value in-

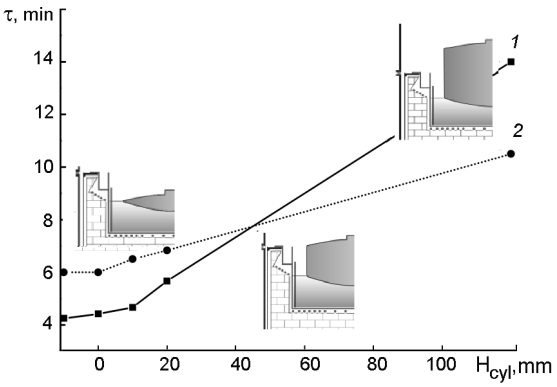

Fig. 5. Thermal lag of upper crystal surface vs. growing crystal dimensions at variation of the bottom (curve *1*) and side heater (curve *2*) temperatures.

creases as compared to the prior stages of crystal growing (see Fig. 2).

The side heater, besides of raw material melting in PCV, heats the furnace atmosphere and growing crystal. In this case, the shorter τ and larger Δt_{pyr} values are observed at PCV wall at heat transfer to closer points. Perhaps this is the cause of shorter τ in all the points (A, A_1 and A_2) at side heater temperature variations.

The results of τ and Δt_{pyr} measurements at crucible are shown in Fig. 4. Those confirm that at short distance between the measurement point and heater, i.e., between the bottom heater and crucible bottom (point B), as well as between the side heater and PCV bottom (point C), temperature changes occur after 4 and 2.5 min, respectively, at maximal Δt_{pyr} values. If the temperature change is recorded in the point B from side heater and in point C from bottom heater, τ in this case is two times larger, while at the same time, Δt_{pyr} values proportionally decrease. The largest temperature change appeared to be for point D at bottom heater temperature variation ($\tau = 10$ min). This result is obvious, since the larger is the distance between points, the longer τ and smaller Δt_{pyr} are, but it confirms the correctness and good sensitivity of our measurements at small temperature variations.

Thus, as the crystal dimensions increase, thermal lag times τ_{bot} and τ_{side} in the point A increase with crystal height according to different laws and $\tau(H_{cyl})$ curves are crossed at the ingot height about 50 mm (Fig. 5). This result can be ascribed to changing spatial arrangement of the measurement point with respect to the heaters (see schemes in Fig. 5).

At initial growth stages, the crystal upper butt is situated at the same height with the side heater, and major part of heat flux therefrom is reflected and scattered to surrounding space of the growth furnace. Then the crystal dimensions increase, and its upper part moves apart from the bottom heater, promoting the proportional τ_{side} decrease and τ_{bot} increase. Herein, at initial stages, the difference between τ_{bot} and τ_{side} is 30 %, then it decreases, changes its sign at $H_{cyl} \approx 50$ mm and reaches −25 % at $H_{cyl} = 120$ mm.

Thus, τ_{bot} increase with H_{cyl} evidences worsening of response rate of the automated crystal diameter control system. The delay of thermal correction pulse may be the cause of volume defects in crystal lattice sometimes appearing in growing crystals [10]. One of possible ways to improvement of the diameter control system is utilization of short-term t_{side} correction starting from $H_{cyl} \approx 50$ mm. This becomes important when the crystal gets out the crucible and heat removal from the crystal increases.

Thus, thermal lag times of growing crystal and the heat assembly elements in dependence on crystal dimensions has been determined experimentally for the first time for CsI(Na) large size crystal grown from constant volume melt on a seed. Thermal lag time at the bottom heater variation is 1.3 times longer than that at the side heater variation. The difference in thermal lag times decreases to zero when crystal gets out the crucible. Then, at further crystal height increase, the $\tau_{bot}-\tau_{side}$ difference changes its sign.

References

1. V.I.Goriletsky, V.A.Nemenov, V.G.Protsenko et al., *J. Cryst. Growth*, **52**, 509 (1981).
2. L.G.Eidelman, V.I.Goriletsky, V.A.Nemenov et al., *Crystal. Res. and Technol.*, **20**, 167 (1985).
3. L.G.Eidelman, V.I.Goriletsky, V.G.Protsenko et al., *J. Crystal Growth*, **128**, 1059 (1993).
4. V.I.Goriletsky, *Izvestiya VUZ, Fizika*, **2**, 38 (2000).
5. V.I.Goriletsky, S.K.Bondarenko, *J. Mat. Sci. &Ing. A.*, **288**, 196 (2000).
6. O.Ts.Sidletskiy, V.I.Goriletsky et al., *Functional Materials*, **12**, 591 (2005).
7. V.I.Goriletsky, O.Ts.Sidletskiy, V.V.Vasilyev, *Functional Materials*, **12**, 765 (2005)
8. V.V.Vasilyev, V.I.Goriletsky, O.Ts.Sidletskiy et al., *Optical Materials*, **30**, 119 (2007)

9. S.K.Bondarenko, V.I.Goriletsky, V.S.Suzdal, *Functional Materials*, **6**, 380 (1999).

10. M.M.Tymoshenko, V.I.Goriletsky, B.V.Grinyov et al., *Crystallography Reports*, **50**, S92 (2005).

Інерційність теплового вузла ростової печі при вирощуванні монокристалів CsI(Na) на запалі із розплаву постійного об'єму

В.І.Горілецький, В.В.Васильєв, О.Ц.Сідлецький, М.М.Тимошенко, В.І.Сумін

Визначено час температурної інерції системи "нагрівач – тигель – кристал" (елементів теплового вузла печі) при вирощуванні крупногабаритних монокристалів CsI(Na) на запалі із розплаву постійного об'єму. Встановлено, що на стадії радіального росту зливка час стабілізації температури при її зміні на донному нагрівачі в 1.3 рази коротше ніж від бічного нагрівача. При аксіальному рості кристала різниця у часі скорочується, потім дорівнює нулю при висоті циліндричної частини ≈50 мм. При подальшому збільшенні висоти кристала ситуація змінюється на протилежну.